Leveraging host metabolism for bisdemethoxycurcumin production in *Pseudomonas putida*

Matthew R. Incha[1,2,3], Mitchell G. Thompson[1,2,3], Jacquelyn M. Blake-Hedges[1,2,4], Allison N. Pearson[1,2], Matthias Schmidt[1,2], Adam M. Deutschbauer[3,5], Jay D. Keasling[1,2,6,7,8]

[1]Joint BioEnergy Institute, 5885 Hollis Street, Emeryville, CA 94608, USA.

[2]Biological Systems & Engineering Division, Lawrence Berkeley National Laboratory, Berkeley, CA 94720, USA.

[3]Department of Plant and Microbial Biology, University of California, Berkeley, CA 94720, USA

[4]Department of Chemistry, University of California, Berkeley, CA 94720, USA

[5]Environmental Genomics and Systems Biology Division, Lawrence Berkeley National Laboratory, Berkeley, California, USA

[6]Department of Chemical and Biomolecular Engineering, University of California, Berkeley, CA 94720, USA

[7]The Novo Nordisk Foundation Center for Biosustainability, Technical University of Denmark, Denmark

[8]Center for Synthetic Biochemistry, Institute for Synthetic Biology, Shenzhen Institutes for Advanced Technologies, Shenzhen, China

ABSTRACT

Pseudomonas putida is a saprophytic bacterium with robust carbon metabolisms and strong solvent tolerance making it an attractive host for metabolic engineering and bioremediation. Due to its diverse carbon metabolisms, its genome encodes an array of proteins and enzymes that can be readily applied to produce valuable products. In this work we sought to identify design principles and bottlenecks in the production of type III polyketide synthase (T3PKS)-derived compounds in *P. putida*. T3PKS products are widely used as nutraceuticals and medicines and often require aromatic starter units, such as coumaroyl-CoA, which is also an intermediate in the native coumarate catabolic pathway of *P. putida*. Using a randomly barcoded transposon mutant (RB-TnSeq) library, we assayed gene functions for a large portion of aromatic catabolism, confirmed known pathways, and proposed new annotations for two aromatic transporters. The tetrahydroxynapthalene synthase of *Streptomyces coelicolor* (RppA), a microbial T3PKS, was then used to rapidly assay growth conditions for increased T3PKS product accumulation. The feruloyl/coumaroyl CoA synthetase (Fcs) of *P. putida* was used to supply coumaroyl-CoA for the curcuminoid synthase (CUS) of *Oryza sativa*, a plant T3PKS. We identified that accumulation of coumaroyl-CoA in this pathway results in extended growth lag times in *P. putida*. Deletion of the second step in coumarate catabolism, the enoyl-CoA hydratase lyase (Ech), resulted in 'drop-in' production of the type III polyketide bisdemethoxycurcumin.

1 INTRODUCTION

Secondary metabolites of fungi, plants, and bacteria have been used as medicines and supplements for millennia [1]. Compounds such as naringenin, raspberry ketone, resveratrol, and curcumin are widely used as nutraceuticals and are biosynthesized through similar pathways

54 [2,3]. Commercially, these chemicals are either extracted directly from plants or produced
55 synthetically, as in the case of raspberry ketone [4]. Renewable microbial production of these
56 compounds will decrease reliance on agriculture and fossil fuel-derived chemical synthesis. The
57 biosynthesis of these compounds (naringenin, raspberry ketone, resveratrol, and curcumin) relies
58 on a class of enzymes called type III polyketide synthases (T3PKSs). T3PKSs carry out iterative
59 Claisen condensation reactions typically with coenzyme A (CoA)-based starter and extender
60 units, both of which vary widely among these enzymes [5]. In the case of the
61 tetrahydroxynapthalene synthase of *Streptomyces coelicolor* (RppA) the starter and extender
62 units are simply malonyl-CoA, while in many plant T3PKSs the starter unit is a
63 phenylpropenoyl-CoA thioester, usually derived from ferulate, coumarate, or cinnamate [6,7].
64 Coumarate and ferulate are components of lignin found in lignocellulosic hydrolysate
65 (LH), which has been proposed for use as a renewable feedstock for biocatalysis [8,9]. However,
66 the limited capabilities of commonly used model organisms, such as *Escherichia coli*, have
67 hindered progress toward making LH a viable feedstock [10]. Characteristics such as high
68 solvent tolerance and diverse carbon metabolisms are lacking in many *E. coli* strains, but are
69 essential for a microbe to be used in LH valorization. With this in mind, it has become apparent
70 that progress needs to be made in developing microbes with these robust traits. Among these
71 emergent organisms is the saprophytic bacterium *Pseudomonas putida. P. putida* has been
72 studied for its ability to catabolize phenolics and withstand solvents, making it an attractive host
73 for LH valorization [11–13].
74 In this work we sought to leverage the native catabolism of *P. putida* KT2440 for use in
75 the biosynthesis of a plant T3PKS product from coumarate. RppA of *S. coelicolor* was first
76 expressed to determine optimal production conditions for T3PKS product accumulation. Next we

77 sought to identify alternative catabolic pathways that could result in reduced titers. Using a
78 randomly barcoded transposon mutant (RB-TnSeq) library of *P. putida*, we assayed for genes
79 involved in the catabolism of coumarate and seven other related aromatic compounds. The native
80 feruloyl/coumaroyl-CoA synthetase (Fcs) of *P. putida* was then used to produce the coumaroyl-
81 CoA starter unit to the curcuminoid synthase (CUS) of *Oryza sativa*. In the process, we found
82 that accumulation of coumaroyl-CoA was toxic to *P. putida*. Finally, relying on the native
83 expression levels of *fcs* from the chromosome and plasmid-based expression of *CUS* resulted in
84 drop-in production of bisdemethoxycurcumin (BDC) from coumarate (Figure 1).

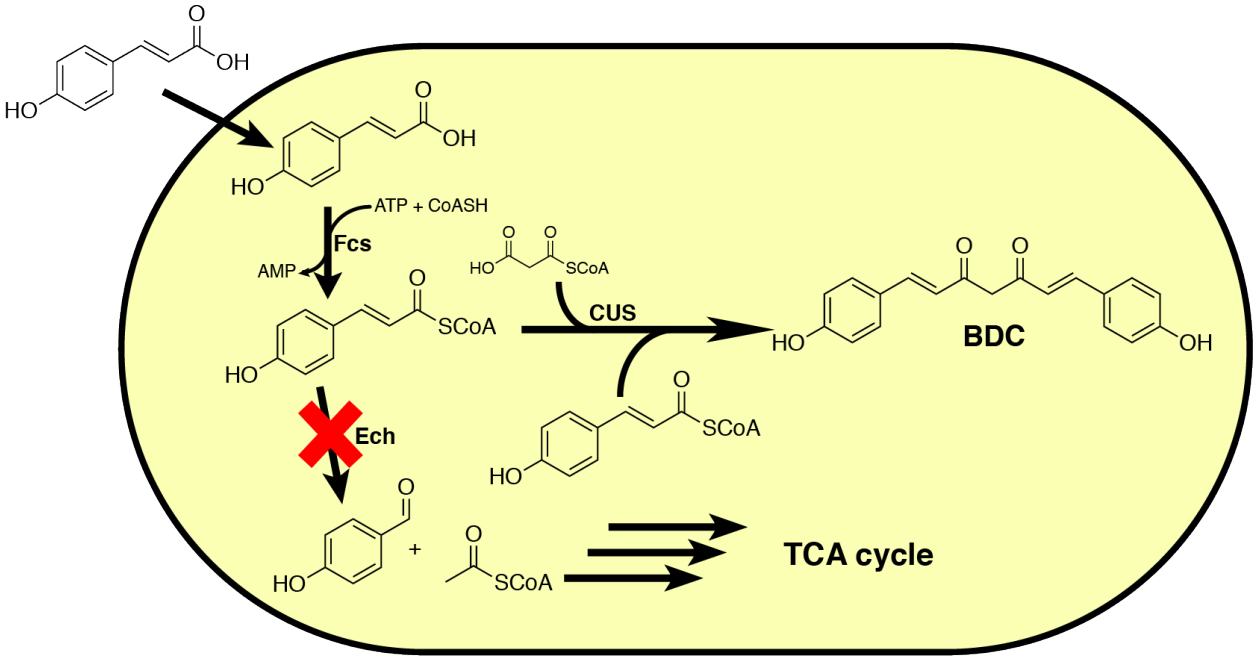

85

86 **Figure 1:** Diagram of the engineered *P. putida* strain used to produce bisdemethoxycurcumin.
87 Fcs is the feruloyl/coumaroyl-CoA synthetase native to *P. putida* KT2440. Ech is the native
88 enoyl-CoA hydratase-lyase which carries out the second step in coumarate catabolism and was
89 knocked out in our production host. CUS is the curcuminoid synthase from *O. sativa.* BDC is the
90 final curcuminoid product, bisdemethoxycurcumin.
91
92 **2 RESULTS**

93 <u>2.1 RppA as a screen for optimal T3PKS production conditions</u>

94 The tetrahydroxynaphthalene synthase of *Streptoyces coelicolor* was recently applied as a
95 biosensor for malonyl-CoA concentrations in several hosts including *P. putida* [14]. We sought
96 to utilize this system to rapidly assay growth conditions for increased T3PKS product
97 accumulation. RppA was initially codon optimized for expression in *P. putida* and cloned into
98 the construct pBADT-*rppA*-OW. We then constructed two more vectors, one with the complete
99 *rppA* cloned from the *S. coelicolor* genome (pBADT-*rppA*-NW) and another with a 5' truncation
100 of 75 base pairs (pBADT-*rppA*-NT) as this had been described previously to increase enzymatic
101 activity [6].

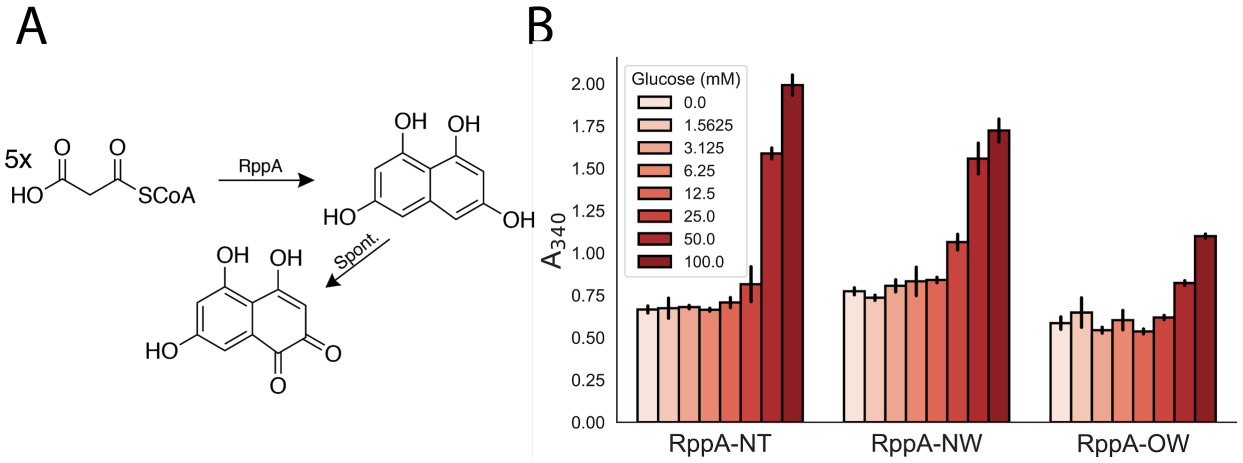

102 **Figure 2:** Flaviolin production as a reference for T3PKS activity. (A) Diagram of the pathway to
103 the red pigment, flaviolin, from RppA and subsequent spontaneous oxidation. (B) Absorbance
104 measurements at 340 nm of supernatants from cells expressing RppA variants in LB containing
105 different concentrations of glucose. Error bars indicate the standard deviation of three trials.
106 RppA-NW contains natural *S. coelicolor* codons, RppA-NT is the same as RppA-NW but with a
107 C-terminal truncation of 25 amino acids, and RppA-OW is translated from a transcript that was
108 codon optimized for *P. putida.*
109
110 Since the product of RppA, 1,3,6,8-tetrahydroxynaphthalene, spontaneously oxidizes to
111 the red pigment flaviolin, we used a colorimetric assay to determine how glucose concentrations
112 affect the production of T3PKS products (Figure 2a). Concentrations of glucose ranging from 0 -
113 100 mM supplemented into LB medium were tested, and the production of flaviolin was

114 measured by absorbance at 340 nm, as previously reported [14]. Unexpectedly, the *rppA*
115 expression vectors using the native *S. coelicolor* codons produced more flaviolin than the *P.*
116 *putida* codon optimized variant (Figure 2b). In all three constructs tested, there was an increase
117 in the accumulation of flaviolin in cultures containing greater than 25 mM glucose (Figure 2b).
118 Given this result, production experiments for bisdemethoxycurcumin were conducted in media
119 supplemented with 100 mM glucose.
120
121

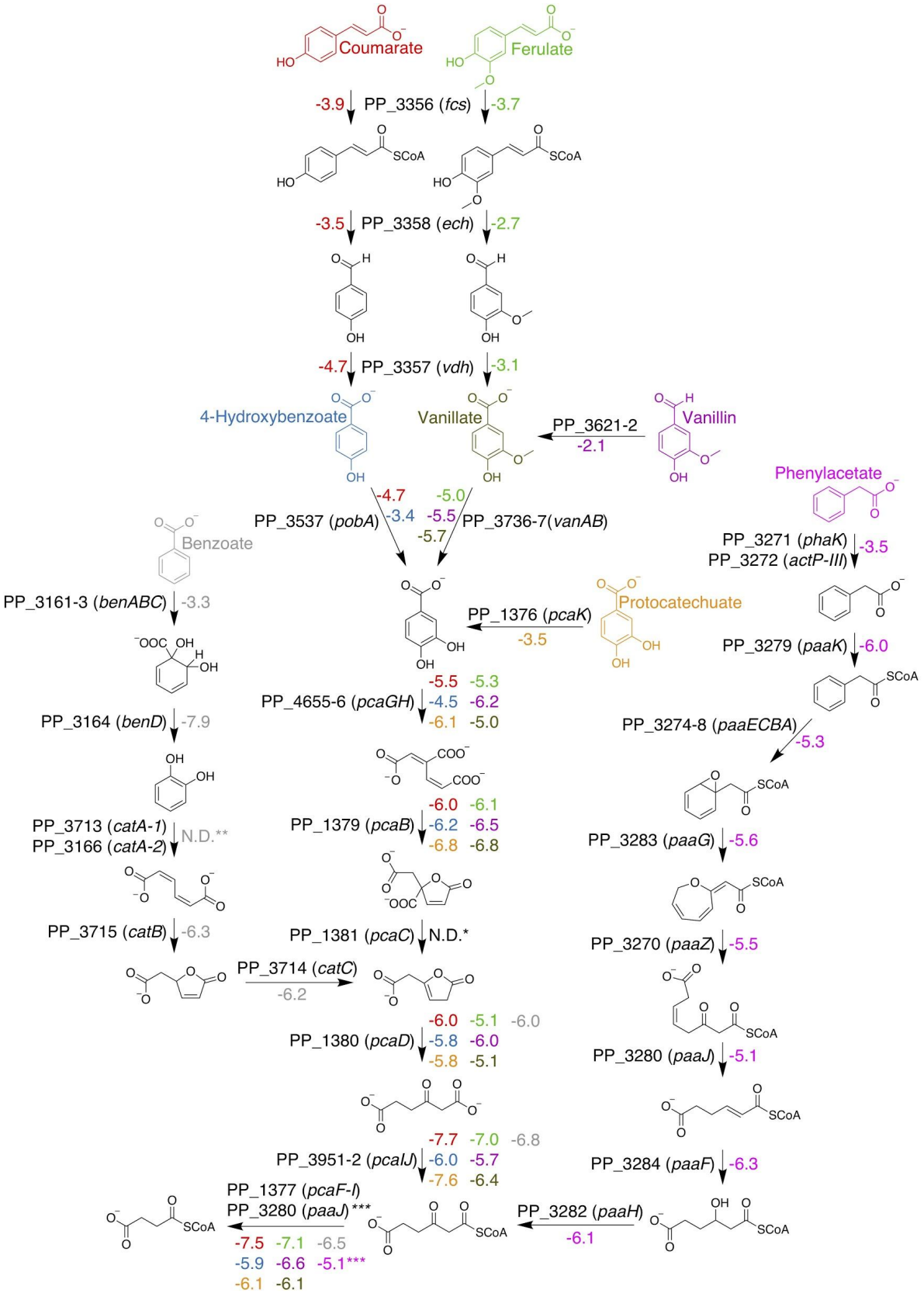
Coumarate
Ferulate
-3.9
PP_3356 (fcs)
-3.7
-3.5
PP_3358 (ech)
-2.7
-4.7
PP_3357 (vdh)
-3.1
4-Hydroxybenzoate
Vanillate
PP_3621-2
-2.1
Vanillin
Phenylacetate
-4.7
-3.4
-5.0
-5.5
-5.7
PP_3537 (pobA)
PP_3736-7(vanAB)
PP_3271 (phaK)
PP_3272 (actP-III)
-3.5
Benzoate
PP_3161-3 (benABC)
-3.3
PP_1376 (pcaK)
-3.5
Protocatechuate
PP_3279 (paaK)
-6.0
-5.5 -5.3
PP_4655-6 (pcaGH)
-4.5 -6.2
-6.1 -5.0
PP_3164 (benD)
-7.9
PP_3274-8 (paaECBA)
-5.3
-6.0 -6.1
PP_3713 (catA-1)
PP_3166 (catA-2)
N.D.**
PP_1379 (pcaB)
-6.2 -6.5
-6.8 -6.8
PP_3283 (paaG)
-5.6
PP_3715 (catB)
-6.3
PP_1381 (pcaC)
N.D.*
PP_3270 (paaZ)
-5.5
PP_3714 (catC)
-6.2
-6.0 -5.1 -6.0
PP_1380 (pcaD)
-5.8 -6.0
-5.8 -5.1
PP_3280 (paaJ)
-5.1
-7.7 -7.0 -6.8
PP_3951-2 (pcaIJ)
-6.0 -5.7
-7.6 -6.4
PP_3284 (paaF)
-6.3
PP_1377 (pcaF-I)
PP_3280 (paaJ)***
PP_3282 (paaH)
-6.1
-7.5 -7.1 -6.5
-5.9 -6.6 -5.1***
-6.1 -6.1

122

Figure 3: Overview of aromatic catabolism in *P. putida* KT2440. The colored and labelled compounds depicted were fed as sole carbon sources to the barcoded transposon library. Fitness values for each gene are the average of 2 replicate RB-TnSeq assays, and are colored corresponding to the carbon source (gray: benzoate, red: coumarate, blue: 4-hydroxybenzoate, light green: ferulate, dark green: vanillate, purple: vanillin, yellow: protocatechuate, pink: phenylacetate). For reactions where multiple genes are necessary, i.e. enzyme complexes, the fitness values for each gene involved in the reaction were averaged. *The t-score for *pcaC* was insignificant ($|t_{score}| < 4.0$) and was excluded from our analysis. **Fitness values for these genes were mild (fitness > -2.0) and excluded. ***Fitness value corresponds to *paaJ*.

2.2 Functional genomics to validate aromatic catabolisms of *P. putida*

While aromatic catabolism has been extensively studied in *P. putida*, genes implicated in these pathways are still being discovered [15]. The genes involved in the first steps of coumarate catabolism reside in an operon with a putative acyl-CoA dehydrogenase (*PP_3354*) and a putative beta-ketothiolase (*PP_3355*), which have been proposed to be involved in an alternative catabolic pathway [16]. As functional redundancy in coumarate catabolism could result in loss of the type III polyketide precursor, coumaroyl-CoA, we sought to identify any pathways that could potentially impact product titers. To assay for genes involved in coumarate and related metabolisms, we grew a randomly barcoded transposon mutant (RB-TnSeq) library of *P. putida* KT2440 in minimal medium with a variety of different aromatic compounds often found in LH (p-coumarate, ferulate, benzoate, p-hydroxybenzoate, protocatechuate, vanillin, vanillate, phenylacetate) and glucose as sole carbon sources. The fitness of each gene was calculated by comparing the abundance of barcodes before versus after growth selection, using barcode sequencing (BarSeq) [17,18]. Negative values indicate that the gene was important for growth in that condition.

The results of the RB-TnSeq assay indicate that the primary route for ferulate and coumarate catabolism is through the feruloyl/coumaroyl-CoA synthetase (Fcs) and the enoyl-CoA hydratase lyase (Ech) (Figure 3 and Figure S1). The genes in the proposed secondary pathway of coumarate and ferulate catabolism, *PP_3354* and *PP_3355*, had no significant fitness

152 phenotype, indicating that these genes are not necessary for coumarate or ferulate catabolism
153 [19].
154 Of all the known reactions depicted in the map of aromatic catabolism (Figure 3), we
155 observed significant negative fitness values for all but three of their corresponding genes: *catA-1*,
156 *catA-2*, and *pcaC*. In the case of *catA-1* and *catA-2* we believe the cause for no fitness phenotype
157 is the functional redundancy of these two genes, i.e. a cell carrying a transposon insertion in one
158 will still have the other gene present. In the case of *pcaC*, we noticed that there was a strong
159 phenotype ($-\log_2 < -2.0$), but the significance fell below our cutoff in all conditions tested ($|t_{score}|$
160 < 4.0). This is likely due to the low frequency of transposon insertions into this gene in the
161 library (n=4). While our results heavily support the current models of aromatic metabolism in *P.*
162 *putida*, our data also indicated that some gene annotations should be revised. *PP_3272* is
163 currently annotated as encoding an acetate permease but given this data and its homology to
164 other systems [20], it should be reannotated as the phenylacetate transporter (phaJ). The
165 *PP_1376* gene is annotated as encoding a 4-hydroxybenzoate transporter; however, we only
166 observed a fitness detriment for this gene with protocatechuate as the sole carbon source.
167 Because of this, *PP_1376* should be reannotated as a protocatechuate transporter.
168 2.3 Accumulation of coumaroyl-CoA is toxic to *P. putida*
169 The first step in the biosynthetic pathway for bisdemethoxycurcumin is the activation of
170 coumarate with coenzyme A (CoASH) (Figure 1). Because *Pseudomonas putida* KT2440
171 natively produces coumaroyl-CoA during coumarate catabolism, we knocked out the subsequent
172 gene in the native catabolic pathway, *ech*, to prevent *P. putida* from consuming this necessary
173 precursor (Figure 1) [20]. Initial production experiments in Δ*ech* strains overexpressing *fcs* and
174 *CUS* from a synthetic operon resulted in an extended lag phase (data not shown). To determine

175 the cause, we overexpressed *fcs* alone under control of the arabinose-inducible *araBAD* promoter

176 (P_{BAD}) in the presence and absence of coumarate (Figure 4A). Increasing the inducer

177 concentration resulted in increased lag times only when coumarate was present in the medium

178 (Figure 4B). This suggested that the coumaroyl-CoA intermediate is toxic to *P. putida*. We

179 therefore sought to minimize the burden of this intermediate by relying on the native

180 chromosomal expression of *fcs* in future experiments.

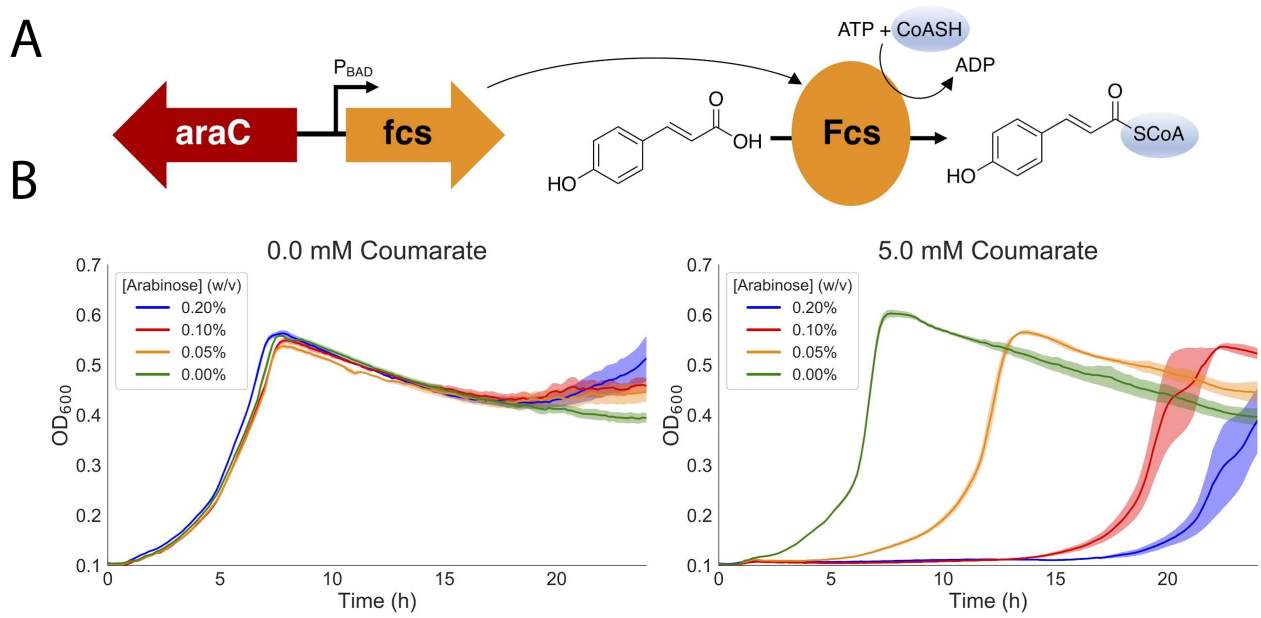

181 **Figure 4:** Production of coumaroyl-CoA inhibits growth of *P. putida.* (A) Diagram of the
182 induction system used to interrogate coumaroyl-CoA toxicity. Fcs was expressed alone from the
183 P_{BAD} promoter and coumarate was added to the media. (B) 24 hour growth curves of KT2440
184 Δ*ech* carrying pBADT-*fcs* in LB induced with varying concentrations of arabinose and no added
185 coumarate (left), or 5 mM coumarate (right). Error bars are +/- the standard deviation of three
186 replicates.
187
188 <u>2.4 Production of bisdemethoxycurcumin</u>

189 In order to produce bisdemethoxycurcumin in *P. putida*, we employed the biochemical

190 pathway outlined in Figure 1. Exogenously added coumarate is activated by the native

191 feruloyl/coumaroyl-CoA synthetase of *P. putida* (Fcs), then two resultant coumaroyl-CoA

192 molecules are condensed with malonyl-CoA by the curcuminoid synthase of *O. sativa* (CUS) to

193 yield bisdemethoxycurcumin [21]. The CoA synthetase, *fcs*, was expressed from its native
194 chromosomal locus, while *CUS* was expressed from the pBADT plasmid and induced with L-
195 arabinose [22].

196 Our initial production strategy was to induce *CUS* until the cultures reached stationary
197 phase. Then the cultures were pelleted and resuspended in fresh LB medium supplemented with
198 5 mM coumarate. These samples were then incubated for another 72 hours. A similar approach
199 had been used successfully in *E. coli* [23]; however, our titers were less than 0.5 mg/L (Figure
200 S2). Given that bisdemethoxycurcumin is insoluble in water [24], a 10 % v/v oleyl alcohol
201 overlay was used to extract the product as the fermentation progressed. Production levels were
202 low (approximately 0.1 mg/L) in *P. putida* Δ*ech* when the medium was supplemented with 10
203 mM coumarate, likely due to the toxicity of coumaroyl-CoA (Figure 5). We therefore lowered
204 the concentration of externally-supplied coumarate in an attempt to decrease precursor toxicity.
205 Supplementation with 5 mM coumarate resulted in a ~5-fold increase in bisdemethoxycurcumin
206 titers in the *P. putida* Δ*ech* strain relative to wild-type (Figure 4A).

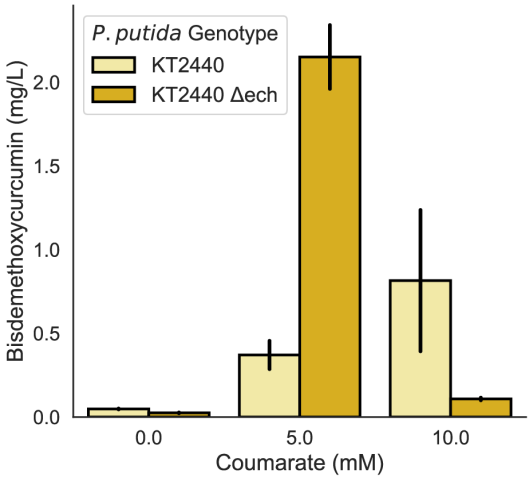

207 **Figure 5**: Bisdemethoxycurcumin titers in *P. putida* KT2440 Δ*ech* and in wildtype KT2440
208 harboring pBADT-CUS. *CUS* was induced with 2 % w/v L-arabinose. Error bars are +/- the
209 standard deviation of three biological replicates.
210

211 **3. DISCUSSION**

212 *Pseudomonas putida* is among the most well studied saprophytic bacteria. Its diverse
213 metabolisms enable it to catabolize a wide variety of complex carbon sources, including
214 lignocellulosic hydrolysate [25]. The robust catabolic pathways of *P. putida*, while useful for
215 producing valuable molecules from diverse carbon sources, can also serve as an obstacle to
216 achieving high product titers as it can often metabolize the desired products [26]. Given recent
217 advances in gene editing techniques [27–31] and our ability to rapidly assay for gene function
218 with transposon site sequencing [17,18,32], engineering non-model hosts like *P. putida* for
219 industrial applications has become less challenging.

220 Using RB-TnSeq mutant fitness assays we were able to rapidly confirm entire pathways
221 of aromatic catabolism (Figure 3 and S1). The genes downstream of *fcs*, previously described as
222 a possible alternative route for coumarate/ferulate catabolism [16,20], showed no significant
223 fitness detriment on any of the carbon sources tested. These genes may be structural remnants of
224 a β-oxidation pathway that eventually evolved into the coumarate/ferulate pathway requiring *fcs*,
225 *ech*, and *vdh* [33]. We then revised the annotations of two genes required for transport of the
226 aromatic compounds, phenylacetate and protocatechuate, an important plant hormone and lignin
227 metabolite respectively [34]. There is a large amount of information in these data about
228 regulatory and structural genetic elements that could be useful to engineers and biologists.

229 Heterologous expression of bacterial T3PKSs, including the tetrahydroxynapthalene
230 synthase of *S. coelicolor* (RppA), has previously been demonstrated in *P. putida* KT2440
231 [14,35,36]. Using variants of *rppA*, we were able to rapidly screen for optimal T3 polyketide
232 production conditions. Expressing the codon optimized variant we created in this study, *rppA*-
233 OW, resulted in less flaviolin production than the native codon variants *rppA*-NW and *rppA*-NT.

234 It is possible that there are some factors affecting heterologous protein expression that are not
235 sufficiently accounted for in current codon optimization algorithms [37]. However, we
236 demonstrated in all our constructs that increasing the glucose concentration had a considerable
237 effect on the production of flaviolin (Figure 2). These T3PKS "sensors" have broad utility in
238 both rapidly assaying culture conditions, as described here, and as high-throughput screens of
239 genetic libraries for increased malonyl-CoA accumulation [14]. Future work could employ these
240 sensors to screen for increased intracellular malonyl-CoA concentrations from a complex
241 substrate like LH.

242 To provide the coumaroyl-CoA substrate for the bisdemethoxycurucumin T3PKS, CUS,
243 we sought to use the native CoA synthetase (Fcs) of *P. putida*. Plasmid-based induction of *fcs*
244 expression in the presence of coumarate, however, resulted in an increase in lag times due to the
245 build up of the toxic coumaroyl-CoA intermediate. This toxicity has been observed in
246 *Acinetobacter baylyi* following disruptions in the gene encoding its enoyl-CoA hydratase lyase
247 and in *E. coli* expressing the *A. baylyi fcs* homolog in the presence of coumarate [38]. This
248 toxicity could also have been limiting other systems using bacterial coumaroyl-CoA synthetases,
249 but the defective growth phenotype may not have been observed due to differences in
250 experimental design [39,40]. The exact cause for coumaroyl-CoA toxicity is unclear and will be
251 the subject of future investigations, as it is likely to interfere with other biosynthetic pathways
252 requiring this intermediate.

253 To engineer *P. putida* for bisdemethoxycurcumin production, we deleted the native
254 enoyl-CoA hydratase lyase (*ech*) responsible for the conversion of coumaroyl-CoA to acetyl-
255 CoA and p-hydroxybenzaldehyde. In order to relieve coumaroyl-CoA toxicity, we relied on the
256 native genomic copy of *fcs* instead of a plasmid-based system. We demonstrated that native

257 expression of *fcs* generates a sufficient coumaroyl-CoA pool for the curcuminoid synthase
258 (CUS). Extraction of the product during growth using an oleyl alcohol overlay also significantly
259 enhanced titers (Figure S2 and 5). In the final *P. putida* production strain, we achieved 'drop-in'
260 production of bisdemethoxycurcumin at titers of 2.15 mg/L (Figure 5).

261 This work is a significant first step towards the production of plant T3PKS-derived
262 compounds in *P. putida*, but several issues remain to be addressed. The use of an overlay and the
263 exogenous addition of coumarate are not feasible for an industrial process. Recent *in vitro* and *in*
264 *vivo* experiments suggest that malonyl-CoA is a limiting factor in plant T3PKS pathways
265 [41,42]. Titers could be improved by modulating this substrate pool. This approach has been
266 successfully used to optimize titers of the T3PKS product naringenin, resulting in titers of 191.9
267 mg/L [35]. Future work could employ a similar strategy in *P. putida* to achieve higher titer
268 production of plant T3PKS products. As we continue to understand more about its metabolism
269 and engineer it more effectively, *P. putida* will become a more attractive host for renewable
270 chemical biosynthesis.

271

272 **4. METHODS**

273 4.1 Media, chemicals, and culture conditions

274 General *E. coli* cultures were grown in Luria-Bertani (LB) Miller medium (BD
275 Biosciences, USA) at 37 °C, while *P. putida* was grown at 30 °C. MOPS minimal media was
276 used where indicated and comprised of the following: 32.5 μM $CaCl_2$, 0.29 mM K_2SO_4, 1.32 mM
277 K_2HPO_4, 8 μM $FeCl_2$, 40 mM MOPS, 4 mM tricine, 0.01 mM $FeSO_4$, 9.52 mM NH_4Cl, 0.52 mM
278 $MgCl_2$, 50 mM NaCl, 0.03 μM $(NH_4)_6Mo_7O_{24}$, 4 μM H_3BO_3, 0.3 μM $CoCl_2$, 0.1 μM $CuSO_4$,
279 0.8 μM $MnCl_2$, and 0.1 μM $ZnSO_4$ [43]. Cultures were supplemented with kanamycin (50 mg/L,

280 Sigma Aldrich, USA) when indicated. Technical grade oleyl alcohol was acquired from Alfa
281 Aesar (Alfa Aesar, Thermo Fisher Scientific). All other compounds were purchased through
282 Sigma Aldrich (Sigma Aldrich, USA). Construction of *P. putida* deletion mutants was performed
283 as described previously [44].

284 4.2 Strains and plasmids

285 Bacterial strains and plasmids used in this work are listed in Table 1. All strains and
286 plasmids created in this work are available through the public instance of the JBEI registry
287 https://public-registry.jbei.org. All plasmids were designed using Device Editor and Vector
288 Editor software, while all primers used for the construction of plasmids were designed using j5
289 software [45–47]. Plasmids were assembled via Gibson Assembly using standard protocols [48],
290 or Golden Gate Assembly using standard protocols [49]. Plasmids were routinely isolated using
291 the Qiaprep Spin Miniprep kit (Qiagen, USA), and all primers were purchased from Integrated
292 DNA Technologies (IDT, Coralville, IA).

293 **Table 1: Strains and plasmids used in this study**

Strain	**JBEI Part ID**	**Reference**
E. coli DH10B		[50]
E. coli BL21(DE3)		Novagen
P. putida KT2440		ATCC 47054
P. putida KT2440 Δ*ech*		Park et al (Unpublished)
Plasmids		

pET28		Novagen
pBADT		[22]
pBADT-*fcs*-*CUS*	TBD	This work
pBADT-*CUS*	TBD	This work
pBADT-*fcs*	TBD	This work
pBADT-*rppA*-NW	TBD	This work
pBADT-*rppA*-NT	TBD	This work
pBADT-*rppA*-OW	TBD	This work
pMQ30		[51]
pMQ30-*PP_3358*		Park et al. (unpublished)

294 4.3 Plate based growth assays

295 Growth studies of bacterial strains were conducted using microplate reader kinetic assays.
296 Overnight cultures were inoculated into 10 mL of LB medium from single colonies, and grown
297 at 30 °C. These cultures were then diluted 1:100 into 500 µL of LB medium with appropriate
298 concentrations of arabinose and p-coumarate in 48-well plates (Falcon, 353072). Plates were
299 sealed with a gas-permeable microplate adhesive film (VWR, USA), and then optical density and
300 fluorescence were monitored for 48 hours in an Biotek Synergy 4 plate reader (BioTek, USA) at
301 30 °C with fast continuous shaking. Optical density was measured at 600 nm.

302 4.4 HPLC detection of bisdemethoxycurcumin

303 HPLC analysis was performed on an Agilent Technologies 1200 series liquid
304 chromatography instrument coupled to a Diode Array Detector (Agilent Technologies, USA).

305 Compounds were separated at a constant flow rate of 0.4 mL/min over a Kinetex C18 column
306 (2.6 µm diameter, 100 Å particle size, dimensions 100 x 3.00 mm, Phenomenex, USA) held at 50
307 °C. The mobile phase consisted of H_2O + 0.1% trifluoroacetic acid (A) and acetonitrile + 0.1%
308 trifluoroacetic acid (B). Separation was performed using the following gradient method: 0-3
309 minutes 95% A, 3-15 minutes 95-5% A, 15-17 minutes 5% A, 17-17.5 minutes 5-95% A, 17.5-
310 20 minutes 95% A. The presence of bisdemethoxycurcumin was monitored and quantified at 440
311 nm.

312 4.5 RB-TnSeq experiments and analysis

313 BarSeq-based experiments utilized the *P. putida* RB-TnSeq library, JBEI-1, which has
314 been described previously [44]. An aliquot of JBEI-1 was thawed on ice, diluted into 25 mL of
315 LB medium supplemented with kanamycin and grown to an OD_{600} of 0.5 at 30 °C. Three 1 mL
316 aliquots of the library were pelleted and stored at -80 °C to later serve as the t_0 of gene
317 abundance. Libraries were then washed in MOPS minimal medium, and diluted 1:50 in MOPS
318 minimal medium with 10 mM p-coumarate, ferulate, benzoate, p-hydroxybenzoate,
319 protocatechuate, vanillin, vanillate, phenylacetate, or D-glucose. Cells were grown in 600 µL of
320 medium in 96-well deep well plates (VWR). Plates were sealed with a gas-permeable microplate
321 adhesive film (VWR, USA), and then grown at 30 °C in an INFORS HT Multitron (Infors USA
322 Inc.), with shaking at 700 rpm. Two 600-µL samples were combined, pelleted, and stored at -
323 80 °C until analysis by BarSeq , which was performed as previously described [17,18]. All
324 fitness data is publically available at http://fit.genomics.lbl.gov.

325 4.5 Curcuminoid production

326 For production of bisdemthoxycurcumin without an overlay, an overnight culture of *P.*
327 *putida* KT2440 Δ*ech* + pBADT-CUS was diluted 1:100 into 5 mL of LB supplemented with 50

328 mg/L kanamycin, 1 % w/v L-arabinose, and 100 mM glucose. The culture was grown to
329 stationary phase over 12 hours then pelleted in a centrifuge at 5000 xg for 5 minutes. The cell
330 pellets were resuspended in 2 mL of fresh LB with 50 mg/L kanamycin, 0.5 % L-arabinose, 100
331 mM glucose, and 5 mM coumarate. The culture was allowed to proceed for 72 hours.

332 Overnights of *P. putida* harboring pBADT-CUS were diluted 1:100 into 25 mL of fresh
333 LB supplemented with 50 mg/L kanamycin, and 100 mM glucose. Arabinose and coumarate
334 were added at the beginning of the fermentation at concentrations indicated. A 2.5 mL overlay of
335 oleyl alcohol was added to extract the bisdemethoxycurcumin during growth. The fermentation
336 was allowed to proceed for 72 hours.

337 4.6 Curcuminoid extraction

338 For cultures lacking an overlay, 0.5 mL of culture was acidified to pH 3 with 3 N HCl.
339 Bisdemethoxycurcumin was then extracted with an equal volume of ethyl acetate. 250 μL of the
340 ethyl acetate layer was removed and the solvent was allowed to evaporate overnight. The dried
341 samples were then resuspended in 50 μL of acetonitrile for analysis with HPLC-DAD.

342 For cultures with an overlay, the cultures were acidified to pH 3 with 3 N HCl. Acidified
343 cultures were then pelleted in a centrifuge and the oleyl alcohol overlays were extracted. To
344 quantify bisdemethoxycurcumin, 100 μL of the extracted overlays were added to a black, clear
345 bottom 96-well plate and absorbance was measured at 425 nm in a Biotek Synergy 4 plate reader
346 (BioTek, USA). A standard curve was made with bisdemethoxycurcumin standards dissolved in
347 oleyl alcohol (Figure S3)

348 4.7 Flaviolin production

349 Colonies of *P. putida* KT2440 strains carrying pBADT-*rppA*-NW, pBADT-*rppA*-NT,
350 and pBADT-*rppA*-OW were used to inoculate LB medium with 50 mg/L kanamycin and

351 cultured overnight. The overnight culture was then diluted 1/100 into fresh LB with 0.2 % w/v L-
352 arabinose, 50 mg/L kanamycin, and 100, 50, 25, 12.5, 6.25, 3.125, 1.5625 or 0 mM glucose.
353 Cultures were conducted in 24-well deep-well plates, and allowed to proceed for 48 hours.
354 Cultures were pelleted in a centrifuge at 5000 xg for 5 minutes. Supernatants were removed,
355 aliquoted into a 96-well black clear bottom plate, and the absorbance was measured at 340 nm in
356 a Biotek Synergy 4 plate reader (BioTek, USA). For cultures expressing *rppA*-NW and *rppA*-NT,
357 the supernatants were too opaque with red product and needed to be diluted 1:2 in fresh LB for
358 accurate absorbance measurements.
359

360 **Acknowledgements**

361 We would like to thank Professor Mattheos Koffas for providing us with the plasmid
362 pEMT6-4CL-CUS. We thank Jesus Barajas for his careful reading of this manuscript and helpful
363 suggestions during preparation. We also thank Morgan Price for assistance in analyzing RB-
364 TnSeq data.

365 This work was part of the DOE Joint BioEnergy Institute (https://www.jbei.org)
366 supported by the U. S. Department of Energy, Office of Science, Office of Biological and
367 Environmental Research, supported by the U.S. Department of Energy, Energy Efficiency and
368 Renewable Energy, Bioenergy Technologies Office, through contract DE-AC02-05CH11231
369 between Lawrence Berkeley National Laboratory and the U.S. Department of Energy. The views
370 and opinions of the authors expressed herein do not necessarily state or reflect those of the
371 United States Government or any agency thereof. Neither the United States Government nor any
372 agency thereof, nor any of their employees, makes any warranty, expressed or implied, or
373 assumes any legal liability or responsibility for the accuracy, completeness, or usefulness of any

information, apparatus, product, or process disclosed, or represents that its use would not infringe privately owned rights. The United States Government retains and the publisher, by accepting the article for publication, acknowledges that the United States Government retains a nonexclusive, paid-up, irrevocable, worldwide license to publish or reproduce the published form of this manuscript, or allow others to do so, for United States Government purposes. The Department of Energy will provide public access to these results of federally sponsored research in accordance with the DOE Public Access Plan (http://energy.gov/downloads/doe-public-access-plan)

Contributions

Conceptualization, M.R.I., M.G.T., J.M.B; Methodology, M.R.I., M.G.T., J.M.B.; Investigation, M.R.I., M.G.T., J.M.B., M.S., A.N.P.; Writing – Original Draft, M.R.I.; Writing – Review and Editing, All authors.; Resources and supervision, A.M.D., J.D.K.

Competing Interests

J.D.K. has financial interests in Amyris, Lygos, Demetrix, Napigen and Maple Bio

Supplementary Figures

Figure S1: Heatmap of RB-TnSeq mutant fitness data. Genes shown have fitness defects ($-\log_2 < -2$) and with statistical significance ($|t_{score}| > 4$) in at least one tested condition which show no significant fitness defects when grown on glucose.

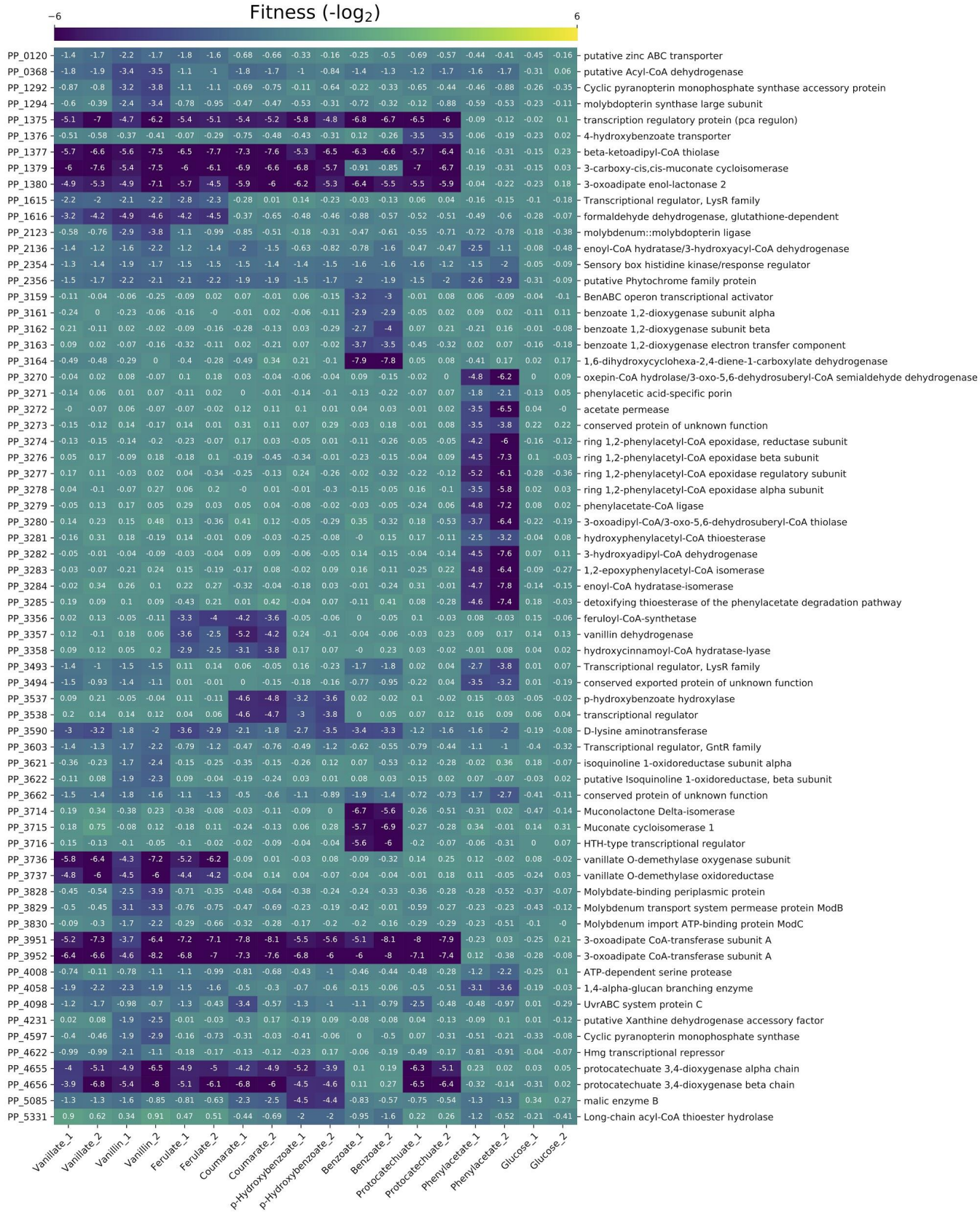
Fitness (-log2)
−6
6
PP_0120 -1.4 -1.7 -2.2 -1.7 -1.8 -1.6 -0.68 -0.66 -0.33 -0.16 -0.25 -0.5 -0.69 -0.57 -0.44 -0.41 -0.45 -0.16 putative zinc ABC transporter
PP_0368 -1.8 -1.9 -3.4 -3.5 -1.1 -1 -1.8 -1.7 -1 -0.84 -1.4 -1.3 -1.2 -1.7 -1.6 -1.7 -0.31 0.06 putative Acyl-CoA dehydrogenase
PP_1292 -0.87 -0.8 -3.2 -3.8 -1.1 -1.1 -0.69 -0.75 -0.11 -0.64 -0.22 -0.33 -0.65 -0.44 -0.46 -0.88 -0.26 -0.35 Cyclic pyranopterin monophosphate synthase accessory protein
PP_1294 -0.6 -0.39 -2.4 -3.4 -0.78 -0.95 -0.47 -0.47 -0.53 -0.31 -0.72 -0.32 -0.12 -0.88 -0.59 -0.53 -0.23 -0.11 molybdopterin synthase large subunit
PP_1375 -5.1 -7 -4.7 -6.2 -5.4 -5.1 -5.4 -5.2 -5.8 -4.8 -6.8 -6.7 -6.5 -6 -0.09 -0.12 -0.02 0.1 transcription regulatory protein (pca regulon)
PP_1376 -0.51 -0.58 -0.37 -0.41 -0.07 -0.29 -0.75 -0.48 -0.43 -0.31 0.12 -0.26 -3.5 -3.5 -0.06 -0.19 -0.23 0.02 4-hydroxybenzoate transporter
PP_1377 -5.7 -6.6 -5.6 -7.5 -6.5 -7.7 -7.3 -7.6 -5.3 -6.5 -6.3 -6.6 -5.7 -6.4 -0.16 -0.31 -0.15 0.23 beta-ketoadipyl-CoA thiolase
PP_1379 -6 -7.6 -5.4 -7.5 -6 -6.1 -6.9 -6.6 -6.8 -5.7 -0.91 -0.85 -7 -6.7 -0.19 -0.31 -0.15 0.03 3-carboxy-cis,cis-muconate cycloisomerase
PP_1380 -4.9 -5.3 -4.9 -7.1 -5.7 -4.5 -5.9 -6 -6.2 -5.3 -6.4 -5.5 -5.5 -5.9 -0.04 -0.22 -0.23 0.18 3-oxoadipate enol-lactonase 2
PP_1615 -2.2 -2 -2.1 -2.2 -2.8 -2.3 -0.28 0.01 0.14 -0.23 -0.03 -0.13 0.06 0.04 -0.16 -0.15 -0.1 -0.18 Transcriptional regulator, LysR family
PP_1616 -3.2 -4.2 -4.9 -4.6 -4.2 -4.5 -0.37 -0.65 -0.48 -0.46 -0.88 -0.57 -0.52 -0.51 -0.49 -0.6 -0.28 -0.07 formaldehyde dehydrogenase, glutathione-dependent
PP_2123 -0.58 -0.76 -2.9 -3.8 -1.1 -0.99 -0.85 -0.51 -0.18 -0.31 -0.47 -0.61 -0.55 -0.71 -0.72 -0.78 -0.18 -0.38 molybdenum::molybdopterin ligase
PP_2136 -1.4 -1.2 -1.6 -2.2 -1.2 -1.4 -2 -1.5 -0.63 -0.82 -0.78 -1.6 -0.47 -0.47 -2.5 -1.1 -0.08 -0.48 enoyl-CoA hydratase/3-hydroxyacyl-CoA dehydrogenase
PP_2354 -1.3 -1.4 -1.9 -1.7 -1.5 -1.5 -1.5 -1.4 -1.4 -1.5 -1.6 -1.6 -1.6 -1.2 -1.5 -2 -0.05 -0.09 Sensory box histidine kinase/response regulator
PP_2356 -1.5 -1.7 -2.2 -2.1 -2.1 -2.2 -1.9 -1.9 -1.5 -1.7 -2 -1.9 -1.5 -2 -2.6 -2.9 -0.31 -0.09 putative Phytochrome family protein
PP_3159 -0.11 -0.04 -0.06 -0.25 -0.09 0.02 0.07 -0.01 0.06 -0.15 -3.2 -3 -0.01 0.08 0.06 -0.09 -0.04 -0.1 BenABC operon transcriptional activator
PP_3161 -0.24 0 -0.23 -0.06 -0.16 -0 -0.01 0.02 -0.06 -0.11 -2.9 -2.9 -0.05 0.02 0.09 0.02 -0.11 0.11 benzoate 1,2-dioxygenase subunit alpha
PP_3162 0.21 -0.11 0.02 -0.02 -0.09 -0.16 -0.28 -0.13 0.03 -0.29 -2.7 -4 0.07 0.21 -0.21 0.16 -0.01 -0.08 benzoate 1,2-dioxygenase subunit beta
PP_3163 0.09 0.02 -0.07 -0.16 -0.32 -0.11 0.02 -0.21 0.07 -0.02 -3.7 -3.5 -0.45 -0.32 0.02 0.07 -0.16 -0.18 benzoate 1,2-dioxygenase electron transfer component
PP_3164 -0.49 -0.48 -0.29 0 -0.4 -0.28 -0.49 0.34 0.21 -0.1 -7.9 -7.8 0.05 0.08 -0.41 0.17 0.02 0.17 1,6-dihydroxycyclohexa-2,4-diene-1-carboxylate dehydrogenase
PP_3270 -0.04 0.02 0.08 -0.07 0.1 0.18 0.03 -0.04 -0.06 -0.04 0.09 -0.15 -0.02 0 -4.8 -6.2 0 0.09 oxepin-CoA hydrolase/3-oxo-5,6-dehydrosuberyl-CoA semialdehyde dehydrogenase
PP_3271 -0.14 0.06 0.01 0.07 -0.11 0.02 0 -0.01 -0.14 -0.1 -0.13 -0.22 -0.07 0.07 -1.8 -2.1 -0.13 0.05 phenylacetic acid-specific porin
PP_3272 -0 -0.07 0.06 -0.07 -0.07 -0.02 0.12 0.11 0.1 0.01 0.04 0.03 -0.01 0.02 -3.5 -6.5 0.04 -0 acetate permease
PP_3273 -0.15 -0.12 0.14 -0.17 0.14 0.01 0.31 0.11 0.07 0.29 -0.03 0.18 -0.01 0.08 -3.5 -3.8 0.22 0.22 conserved protein of unknown function
PP_3274 -0.13 -0.15 -0.14 -0.2 -0.23 -0.07 0.17 0.03 -0.05 0.01 -0.11 -0.26 -0.05 -0.05 -4.2 -6 -0.16 -0.12 ring 1,2-phenylacetyl-CoA epoxidase, reductase subunit
PP_3276 0.05 0.17 -0.09 0.18 -0.18 0.1 -0.19 -0.45 -0.34 -0.01 -0.23 -0.15 -0.04 0.09 -4.5 -7.3 0.1 -0.03 ring 1,2-phenylacetyl-CoA epoxidase beta subunit
PP_3277 0.17 0.11 -0.03 0.02 0.04 -0.34 -0.25 -0.13 0.24 -0.26 -0.02 -0.32 -0.22 -0.12 -5.2 -6.1 -0.28 -0.36 ring 1,2-phenylacetyl-CoA epoxidase regulatory subunit
PP_3278 0.04 -0.1 -0.07 0.27 0.06 0.2 -0 0.01 -0.01 -0.3 -0.15 -0.05 0.16 -0.1 -3.5 -5.8 0.02 0.03 ring 1,2-phenylacetyl-CoA epoxidase alpha subunit
PP_3279 -0.05 0.13 0.17 0.05 0.29 0.03 0.05 0.04 -0.08 -0.02 -0.03 -0.05 -0.24 0.06 -4.8 -7.2 0.08 0.02 phenylacetate-CoA ligase
PP_3280 0.14 0.23 0.15 0.48 0.13 -0.36 0.41 0.12 -0.05 -0.29 0.35 -0.32 0.18 -0.53 -3.7 -6.4 -0.22 -0.19 3-oxoadipyl-CoA/3-oxo-5,6-dehydrosuberyl-CoA thiolase
PP_3281 -0.16 0.31 0.18 -0.19 0.14 -0.01 0.09 -0.03 -0.25 -0.08 -0 0.15 0.17 -0.11 -2.5 -3.2 -0.04 0.08 hydroxyphenylacetyl-CoA thioesterase
PP_3282 -0.05 -0.01 -0.04 -0.09 -0.03 -0.04 0.09 0.09 -0.06 -0.05 0.14 -0.15 -0.04 -0.14 -4.5 -7.6 0.07 0.11 3-hydroxyadipyl-CoA dehydrogenase
PP_3283 -0.03 -0.07 -0.21 0.24 0.15 -0.19 -0.17 0.08 -0.02 0.09 0.16 -0.11 -0.25 0.22 -4.8 -6.4 -0.09 -0.27 1,2-epoxyphenylacetyl-CoA isomerase
PP_3284 -0.02 0.34 0.26 0.1 0.22 0.27 -0.32 -0.04 -0.18 0.03 -0.01 -0.24 0.31 -0.01 -4.7 -7.8 -0.14 -0.15 enoyl-CoA hydratase-isomerase
PP_3285 0.19 0.09 0.1 0.09 -0.43 0.21 0.01 0.42 -0.04 0.07 -0.11 0.41 0.08 -0.28 -4.6 -7.4 0.18 -0.03 detoxifying thioesterase of the phenylacetate degradation pathway
PP_3356 0.02 0.13 -0.05 -0.11 -3.3 -4 -4.2 -3.6 -0.05 -0.06 0 -0.05 0.1 -0.03 0.08 -0.03 0.15 -0.06 feruloyl-CoA-synthetase
PP_3357 0.12 -0.1 0.18 0.06 -3.6 -2.5 -5.2 -4.2 0.24 -0.1 -0.04 -0.06 -0.03 0.23 0.09 0.17 0.14 0.13 vanillin dehydrogenase
PP_3358 0.09 0.12 0.05 0.2 -2.9 -2.5 -3.1 -3.8 0.17 0.07 -0 0.23 0.03 -0.02 -0.01 0.08 0.04 0.02 hydroxycinnamoyl-CoA hydratase-lyase
PP_3493 -1.4 -1 -1.5 -1.5 0.11 0.14 0.06 -0.05 0.16 -0.23 -1.7 -1.8 0.02 0.04 -2.7 -3.8 0.01 0.07 Transcriptional regulator, LysR family
PP_3494 -1.5 -0.93 -1.4 -1.1 0.01 -0.01 0 -0.15 -0.18 -0.16 -0.77 -0.95 -0.22 0.04 -3.5 -3.2 0.01 -0.19 conserved exported protein of unknown function
PP_3537 0.09 0.21 -0.05 -0.04 0.11 -0.11 -4.6 -4.8 -3.2 -3.6 0.02 -0.02 0.1 -0.02 0.15 -0.03 -0.05 -0.02 p-hydroxybenzoate hydroxylase
PP_3538 0.2 0.14 0.14 0.12 0.04 0.06 -4.6 -4.7 -3 -3.8 0 0.05 0.07 0.12 0.16 0.09 0.06 0.04 transcriptional regulator
PP_3590 -3 -3.2 -1.8 -2 -3.6 -2.9 -2.1 -1.8 -2.7 -3.5 -3.4 -3.3 -1.2 -1.6 -1.6 -2 -0.19 -0.08 D-lysine aminotransferase
PP_3603 -1.4 -1.3 -1.7 -2.2 -0.79 -1.2 -0.47 -0.76 -0.49 -1.2 -0.62 -0.55 -0.79 -0.44 -1.1 -1 -0.4 -0.32 Transcriptional regulator, GntR family
PP_3621 -0.36 -0.23 -1.7 -2.4 -0.15 -0.25 -0.35 -0.15 -0.26 0.12 0.07 -0.53 -0.12 -0.28 -0.02 0.36 0.18 -0.07 isoquinoline 1-oxidoreductase subunit alpha
PP_3622 -0.11 0.08 -1.9 -2.3 0.09 -0.04 -0.19 -0.24 0.03 0.01 0.08 0.03 -0.15 0.02 0.07 -0.07 -0.03 0.02 putative Isoquinoline 1-oxidoreductase, beta subunit
PP_3662 -1.5 -1.4 -1.8 -1.6 -1.1 -1.3 -0.5 -0.6 -1.1 -0.89 -1.9 -1.4 -0.72 -0.73 -1.7 -2.7 -0.41 -0.11 conserved protein of unknown function
PP_3714 0.19 0.34 -0.38 0.23 -0.38 -0.08 -0.03 -0.11 -0.09 0 -6.7 -5.6 -0.26 -0.51 -0.31 0.02 -0.47 -0.14 Muconolactone Delta-isomerase
PP_3715 0.18 0.75 -0.08 0.12 -0.18 0.11 -0.24 -0.13 0.06 0.28 -5.7 -6.9 -0.27 -0.28 0.34 -0.01 0.14 0.31 Muconate cycloisomerase 1
PP_3716 0.15 -0.13 -0.1 -0.05 -0.1 -0.02 -0.02 -0.09 -0.04 -0.04 -5.6 -6 -0.2 -0.07 -0.06 -0.31 0 0.07 HTH-type transcriptional regulator
PP_3736 -5.8 -6.4 -4.3 -7.2 -5.2 -6.2 -0.09 0.01 -0.03 0.08 -0.09 -0.32 0.14 0.25 0.12 -0.02 0.08 -0.02 vanillate O-demethylase oxygenase subunit
PP_3737 -4.8 -6 -4.5 -6 -4.4 -4.2 -0.04 0.14 0.04 -0.07 -0.04 -0.04 -0.01 0.18 0.11 -0.05 -0.24 0.03 vanillate O-demethylase oxidoreductase
PP_3828 -0.45 -0.54 -2.5 -3.9 -0.71 -0.35 -0.48 -0.64 -0.38 -0.24 -0.24 -0.33 -0.36 -0.28 -0.28 -0.52 -0.37 -0.07 Molybdate-binding periplasmic protein
PP_3829 -0.5 -0.45 -3.1 -3.3 -0.76 -0.75 -0.47 -0.69 -0.23 -0.19 -0.42 -0.01 -0.59 -0.27 -0.23 -0.23 -0.43 -0.12 Molybdenum transport system permease protein ModB
PP_3830 -0.09 -0.3 -1.7 -2.2 -0.29 -0.66 -0.32 -0.28 -0.17 -0.2 -0.2 -0.16 -0.29 -0.29 -0.23 -0.51 -0.1 -0 Molybdenum import ATP-binding protein ModC
PP_3951 -5.2 -7.3 -3.7 -6.4 -7.2 -7.1 -7.8 -8.1 -5.5 -5.6 -5.1 -8.1 -8 -7.9 -0.23 0.03 -0.25 0.21 3-oxoadipate CoA-transferase subunit A
PP_3952 -6.4 -6.6 -4.6 -8.2 -6.8 -7 -7.3 -7.6 -6.8 -6 -6 -8 -7.1 -7.4 0.12 -0.38 -0.28 -0.08 3-oxoadipate CoA-transferase subunit A
PP_4008 -0.74 -0.11 -0.78 -1.1 -1.1 -0.99 -0.81 -0.68 -0.43 -1 -0.46 -0.44 -0.48 -0.28 -1.2 -2.2 -0.25 0.1 ATP-dependent serine protease
PP_4058 -1.9 -2.2 -2.3 -1.9 -1.5 -1.6 -0.5 -0.3 -0.7 -0.6 -0.15 -0.06 -0.5 -0.51 -3.1 -3.6 -0.19 -0.03 1,4-alpha-glucan branching enzyme
PP_4098 -1.2 -1.7 -0.98 -0.7 -1.3 -0.43 -3.4 -0.57 -1.3 -1 -1.1 -0.79 -2.5 -0.48 -0.48 -0.97 0.01 -0.29 UvrABC system protein C
PP_4231 0.02 0.08 -1.9 -2.5 -0.01 -0.03 -0.3 0.17 -0.19 0.09 -0.08 -0.08 0.04 -0.13 -0.09 0.1 0.01 -0.12 putative Xanthine dehydrogenase accessory factor
PP_4597 -0.4 -0.46 -1.9 -2.9 -0.16 -0.73 -0.31 -0.03 -0.41 -0.06 0 -0.5 0.07 -0.31 -0.51 -0.21 -0.33 -0.08 Cyclic pyranopterin monophosphate synthase
PP_4622 -0.99 -0.99 -2.1 -1.1 -0.18 -0.17 -0.13 -0.12 -0.23 0.17 -0.06 -0.19 -0.49 -0.17 -0.81 -0.91 -0.04 -0.07 Hmg transcriptional repressor
PP_4655 -4 -5.1 -4.9 -6.5 -4.9 -5 -4.2 -4.9 -5.2 -3.9 0.1 0.19 -6.3 -5.1 0.23 0.02 0.03 0.05 protocatechuate 3,4-dioxygenase alpha chain
PP_4656 -3.9 -6.8 -5.4 -8 -5.1 -6.1 -6.8 -6 -4.5 -4.6 0.11 0.27 -6.5 -6.4 -0.32 -0.14 -0.31 0.02 protocatechuate 3,4-dioxygenase beta chain
PP_5085 -1.3 -1.3 -1.6 -0.85 -0.81 -0.63 -2.3 -2.5 -4.5 -4.4 -0.83 -0.57 -0.75 -0.54 -1.3 -1.3 0.34 0.27 malic enzyme B
PP_5331 0.9 0.62 0.34 0.91 0.47 0.51 -0.44 -0.69 -2 -2 -0.95 -1.6 0.22 0.26 -1.2 -0.52 -0.21 -0.41 Long-chain acyl-CoA thioester hydrolase
Vanillate_1
Vanillate_2
Vanillin_1
Vanillin_2
Ferulate_1
Ferulate_2
Coumarate_1
Coumarate_2
p-Hydroxybenzoate_1
p-Hydroxybenzoate_2
Benzoate_1
Benzoate_2
Protocatechuate_1
Protocatechuate_2
Phenylacetate_1
Phenylacetate_2
Glucose_1
Glucose_2

Figure S2: HPLC trace of curcumin extracted from *P. putida* KT2440 Δ*ech* + pBADT-CUS overlaid with a 3.125 mg/L standard

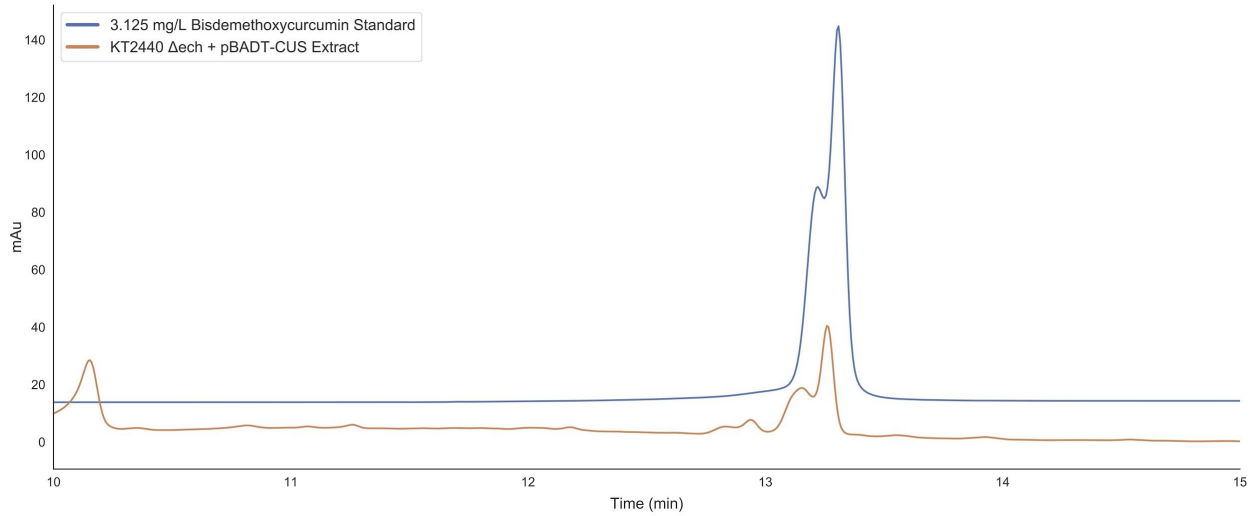

Figure S3: Standard curve of bisdemethoxycurcumin. Absorbance measurements at 425 nm from 50 to 0 mg/L of bisdemethoxycurcumin dissolved in oleyl alcohol.

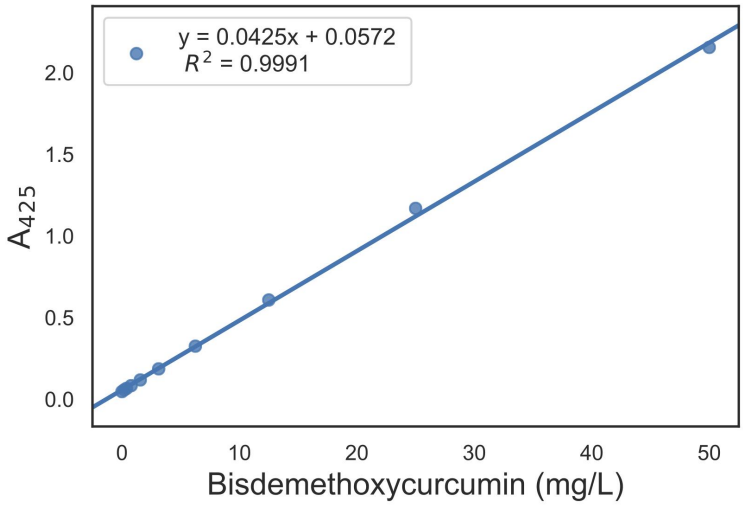

Bibliography

[1] S.J. Hewlings, D.S. Kalman, Curcumin: A review of its' effects on human health., Foods. 6 (2017). doi:10.3390/foods6100092.

[2] S. Schanz, G. Schröder, J. Schröder, Stilbene synthase from Scots pine (*Pinus sylvestris*), FEBS Lett. 313 (1992) 71–74. doi:10.1016/0014-5793(92)81187-Q.

[3] W. Heller, K. Hahlbrock, Highly purified "flavanone synthase" from parsley catalyzes the formation of naringenin chalcone, Arch. Biochem. Biophys. 200 (1980) 617–619. doi:10.1016/0003-9861(80)90395-1.

[4] L.R. Smith, Rheosmin ("Raspberry Ketone") and Zingerone, and Their Preparation

412 by Crossed Aldol-Catalytic Hydrogenation Sequences, Chem. Educator. 1 (1996) 1–
413 18. doi:10.1007/s00897960034a.
414 [5] D. Yu, F. Xu, J. Zeng, J. Zhan, Type III polyketide synthases in natural product
415 biosynthesis., IUBMB Life. 64 (2012) 285–295. doi:10.1002/iub.1005.
416 [6] M. Izumikawa, P.R. Shipley, J.N. Hopke, T. O'Hare, L. Xiang, J.P. Noel, et al.,
417 Expression and characterization of the type III polyketide synthase 1,3,6,8-
418 tetrahydroxynaphthalene synthase from Streptomyces coelicolor A3(2)., J. Ind.
419 Microbiol. Biotechnol. 30 (2003) 510–515. doi:10.1007/s10295-003-0075-8.
420 [7] T. Wakimoto, H. Morita, I. Abe, Engineering of plant type III polyketide synthases.,
421 Meth. Enzymol. 515 (2012) 337–358. doi:10.1016/B978-0-12-394290-6.00016-1.
422 [8] J.M. Lawther, R. Sun, The fractional characterisation of polysaccharides and lignin
423 components in alkaline treated and atmospheric refined wheat straw, Industrial
424 Crops and Products. 5 (1996) 87–95. doi:10.1016/0926-6690(96)00002-7.
425 [9] L.J. Jönsson, B. Alriksson, N.-O. Nilvebrant, Bioconversion of lignocellulose:
426 inhibitors and detoxification., Biotechnol. Biofuels. 6 (2013) 16. doi:10.1186/1754-
427 6834-6-16.
428 [10] T.Y. Mills, N.R. Sandoval, R.T. Gill, Cellulosic hydrolysate toxicity and tolerance
429 mechanisms in Escherichia coli., Biotechnol. Biofuels. 2 (2009) 26. doi:10.1186/1754-
430 6834-2-26.
431 [11] T. Nakazawa, T. Yokota, Benzoate metabolism in Pseudomonas putida(arvilla) mt-
432 2: demonstration of two benzoate pathways., J. Bacteriol. 115 (1973) 262–267.
433 [12] M.T. Guarnieri, M. Ann Franden, C.W. Johnson, G.T. Beckham, Conversion and
434 assimilation of furfural and 5-(hydroxymethyl)furfural by Pseudomonas putida
435 KT2440., Metab. Eng. Commun. 4 (2017) 22–28. doi:10.1016/j.meteno.2017.02.001.
436 [13] J.G. Linger, D.R. Vardon, M.T. Guarnieri, E.M. Karp, G.B. Hunsinger, M.A.
437 Franden, et al., Lignin valorization through integrated biological funneling and
438 chemical catalysis., Proc Natl Acad Sci USA. 111 (2014) 12013–12018.
439 doi:10.1073/pnas.1410657111.
440 [14] D. Yang, W.J. Kim, S.M. Yoo, J.H. Choi, S.H. Ha, M.H. Lee, et al., Repurposing
441 type III polyketide synthase as a malonyl-CoA biosensor for metabolic engineering in
442 bacteria., Proc Natl Acad Sci USA. 115 (2018) 9835–9844.
443 doi:10.1073/pnas.1808567115.
444 [15] M.N. Price, J. Ray, A.T. Iavarone, H.K. Carlson, E.M. Ryan, R.R. Malmstrom, et
445 al., Oxidative pathways of deoxyribose and deoxyribonate catabolism., MSystems. 4
446 (2019). doi:10.1128/mSystems.00297-18.
447 [16] J. Overhage, H. Priefert, J. Rabenhorst, A. Steinbüchel, Biotransformation of
448 eugenol to vanillin by a mutant of Pseudomonas sp. strain HR199 constructed by
449 disruption of the vanillin dehydrogenase (vdh) gene, Appl. Microbiol. Biotechnol.
450 52 (1999) 820–828. doi:10.1007/s002530051598.
451 [17] K.M. Wetmore, M.N. Price, R.J. Waters, J.S. Lamson, J. He, C.A. Hoover, et al.,

452 **Rapid quantification of mutant fitness in diverse bacteria by sequencing randomly**
453 **bar-coded transposons., MBio. 6 (2015) e00306-15. doi:10.1128/mBio.00306-15.**
454 **[18] J.M. Rand, T. Pisithkul, R.L. Clark, J.M. Thiede, C.R. Mehrer, D.E. Agnew, et al.,**
455 **A metabolic pathway for catabolizing levulinic acid in bacteria., Nat. Microbiol. 2**
456 **(2017) 1624–1634. doi:10.1038/s41564-017-0028-z.**
457 **[19] R. Plaggenborg, J. Overhage, A. Steinbüchel, H. Priefert, Functional analyses of**
458 **genes involved in the metabolism of ferulic acid in Pseudomonas putida KT2440.,**
459 **Appl. Microbiol. Biotechnol. 61 (2003) 528–535. doi:10.1007/s00253-003-1260-4.**
460 **[20] J.I. Jiménez, B. Miñambres, J.L. García, E. Díaz, Genomic analysis of the aromatic**
461 **catabolic pathways from Pseudomonas putida KT2440., Environ. Microbiol. 4 (2002)**
462 **824–841. doi:10.1046/j.1462-2920.2002.00370.x.**
463 **[21] Y. Katsuyama, M. Matsuzawa, N. Funa, S. Horinouchi, In vitro synthesis of**
464 **curcuminoids by type III polyketide synthase from Oryza sativa., J. Biol. Chem. 282**
465 **(2007) 37702–37709. doi:10.1074/jbc.M707569200.**
466 **[22] C. Bi, P. Su, J. Müller, Y.-C. Yeh, S.R. Chhabra, H.R. Beller, et al., Development of**
467 **a broad-host synthetic biology toolbox for Ralstonia eutropha and its application to**
468 **engineering hydrocarbon biofuel production., Microb. Cell Fact. 12 (2013) 107.**
469 **doi:10.1186/1475-2859-12-107.**
470 **[23] Y. Katsuyama, N. Funa, I. Miyahisa, S. Horinouchi, Synthesis of unnatural**
471 **flavonoids and stilbenes by exploiting the plant biosynthetic pathway in Escherichia**
472 **coli., Chem. Biol. 14 (2007) 613–621. doi:10.1016/j.chembiol.2007.05.004.**
473 **[24] I. Javeri, N. Chand, Curcumin, in: Nutraceuticals, Elsevier, 2016: pp. 435–445.**
474 **doi:10.1016/B978-0-12-802147-7.00031-0.**
475 **[25] Y. Wang, F. Horlamus, M. Henkel, F. Kovacic, S. Schläfle, R. Hausmann, et al.,**
476 **Growth of engineered*Pseudomonas putida* KT2440 on glucose, xylose and arabinose:**
477 **hemicellulose hydrolysates and their major sugars as sustainable carbon sources,**
478 **Glob. Change Biol. Bioenergy. (2019). doi:10.1111/gcbb.12590.**
479 **[26] M.G. Thompson, L.E. Valencia, J.M. Blake-Hedges, P. Cruz-Morales, A.E.**
480 **Velasquez, A.N. Pearson, et al., Omics-driven identification and elimination of**
481 **valerolactam catabolism in Pseudomonas putida KT2440 for increased product titer,**
482 **Metab. Eng. Commun. (2019) e00098. doi:10.1016/j.mec.2019.e00098.**
483 **[27] T.B. Cook, J.M. Rand, W. Nurani, D.K. Courtney, S.A. Liu, B.F. Pfleger, Genetic**
484 **tools for reliable gene expression and recombineering in Pseudomonas putida., J.**
485 **Ind. Microbiol. Biotechnol. 45 (2018) 517–527. doi:10.1007/s10295-017-2001-5.**
486 **[28] T. Aparicio, V. de Lorenzo, E. Martínez-García, CRISPR/Cas9-Based**
487 **Counterselection Boosts Recombineering Efficiency in Pseudomonas putida.,**
488 **Biotechnol. J. 13 (2018) e1700161. doi:10.1002/biot.201700161.**
489 **[29] T. Aparicio, V. de Lorenzo, E. Martínez-García, CRISPR/Cas9-enhanced ssDNA**
490 **recombineering for Pseudomonas putida., Microb. Biotechnol. 12 (2019) 1076–1089.**
491 **doi:10.1111/1751-7915.13453.**

492 [30] E. Martínez-García, V. de Lorenzo, Engineering multiple genomic deletions in
493 Gram-negative bacteria: analysis of the multi-resistant antibiotic profile of
494 Pseudomonas putida KT2440., Environ. Microbiol. 13 (2011) 2702–2716.
495 doi:10.1111/j.1462-2920.2011.02538.x.
496 [31] N.T. Wirth, E. Kozaeva, P.I. Nikel, Accelerated genome engineering of
497 Pseudomonas putida by I-SceI-mediated recombination and CRISPR-Cas9
498 counterselection., Microb. Biotechnol. (2019). doi:10.1111/1751-7915.13396.
499 [32] M.N. Price, K.M. Wetmore, R.J. Waters, M. Callaghan, J. Ray, H. Liu, et al.,
500 Mutant phenotypes for thousands of bacterial genes of unknown function., Nature.
501 557 (2018) 503–509. doi:10.1038/s41586-018-0124-0.
502 [33] H. Priefert, J. Rabenhorst, A. Steinbüchel, Biotechnological production of vanillin.,
503 Appl. Microbiol. Biotechnol. 56 (2001) 296–314. doi:10.1007/s002530100687.
504 [34] F. Wightman, D.L. Lighty, Identification of phenylacetic acid as a natural auxin in
505 the shoots of higher plants, Physiol. Plant. 55 (1982) 17–24. doi:10.1111/j.1399-
506 3054.1982.tb00278.x.
507 [35] S. Zhou, Y. Lyu, H. Li, M.A.G. Koffas, J. Zhou, Fine-tuning the (2S)-naringenin
508 synthetic pathway using an iterative high-throughput balancing strategy.,
509 Biotechnol. Bioeng. 116 (2019) 1392–1404. doi:10.1002/bit.26941.
510 [36] A. Martinez, S.J. Kolvek, C.L.T. Yip, J. Hopke, K.A. Brown, I.A. MacNeil, et al.,
511 Genetically modified bacterial strains and novel bacterial artificial chromosome
512 shuttle vectors for constructing environmental libraries and detecting heterologous
513 natural products in multiple expression hosts., Appl. Environ. Microbiol. 70 (2004)
514 2452–2463. doi:10.1128/aem.70.4.2452-2463.2004.
515 [37] G. Cambray, J.C. Guimaraes, A.P. Arkin, Evaluation of 244,000 synthetic sequences
516 reveals design principles to optimize translation in Escherichia coli., Nat. Biotechnol.
517 36 (2018) 1005–1015. doi:10.1038/nbt.4238.
518 [38] D. Parke, L.N. Ornston, Toxicity caused by hydroxycinnamoyl-coenzyme A
519 thioester accumulation in mutants of Acinetobacter sp. strain ADP1., Appl. Environ.
520 Microbiol. 70 (2004) 2974–2983.
521 [39] C.N.S. Santos, M. Koffas, G. Stephanopoulos, Optimization of a heterologous
522 pathway for the production of flavonoids from glucose., Metab. Eng. 13 (2011) 392–
523 400. doi:10.1016/j.ymben.2011.02.002.
524 [40] S.R. Park, J.A. Yoon, J.H. Paik, J.W. Park, W.S. Jung, Y.-H. Ban, et al.,
525 Engineering of plant-specific phenylpropanoids biosynthesis in Streptomyces
526 venezuelae., J. Biotechnol. 141 (2009) 181–188. doi:10.1016/j.jbiotec.2009.03.013.
527 [41] Y. Zang, J. Zha, X. Wu, Z. Zheng, J. Ouyang, M.A.G. Koffas, In Vitro Naringenin
528 Biosynthesis from p-Coumaric Acid Using Recombinant Enzymes., J. Agric. Food
529 Chem. (2019). doi:10.1021/acs.jafc.9b00413.
530 [42] Z. Fang, J.A. Jones, J. Zhou, M.A.G. Koffas, Engineering Escherichia coli Co-
531 Cultures for Production of Curcuminoids From Glucose., Biotechnol. J. 13 (2018)

532 e1700576. doi:10.1002/biot.201700576.
533 [43] A.E. LaBauve, M.J. Wargo, Growth and laboratory maintenance of Pseudomonas
534 aeruginosa., Curr. Protoc. Microbiol. Chapter 6 (2012) Unit 6E.1.
535 doi:10.1002/9780471729259.mc06e01s25.
536 [44] M.G. Thompson, J.M. Blake-Hedges, P. Cruz-Morales, J.F. Barajas, S.C. Curran,
537 C.B. Eiben, et al., Massively Parallel Fitness Profiling Reveals Multiple Novel
538 Enzymes in Pseudomonas putida Lysine Metabolism., MBio. 10 (2019).
539 doi:10.1128/mBio.02577-18.
540 [45] T.S. Ham, Z. Dmytriv, H. Plahar, J. Chen, N.J. Hillson, J.D. Keasling, Design,
541 implementation and practice of JBEI-ICE: an open source biological part registry
542 platform and tools., Nucleic Acids Res. 40 (2012) e141. doi:10.1093/nar/gks531.
543 [46] J. Chen, D. Densmore, T.S. Ham, J.D. Keasling, N.J. Hillson, DeviceEditor visual
544 biological CAD canvas., J. Biol. Eng. 6 (2012) 1. doi:10.1186/1754-1611-6-1.
545 [47] N.J. Hillson, R.D. Rosengarten, J.D. Keasling, j5 DNA assembly design automation
546 software., ACS Synth. Biol. 1 (2012) 14–21. doi:10.1021/sb2000116.
547 [48] D.G. Gibson, L. Young, R.-Y. Chuang, J.C. Venter, C.A. Hutchison, H.O. Smith,
548 Enzymatic assembly of DNA molecules up to several hundred kilobases., Nat.
549 Methods. 6 (2009) 343–345. doi:10.1038/nmeth.1318.
550 [49] C. Engler, R. Kandzia, S. Marillonnet, A one pot, one step, precision cloning method
551 with high throughput capability., PLoS ONE. 3 (2008) e3647.
552 doi:10.1371/journal.pone.0003647.
553 [50] S.G. Grant, J. Jessee, F.R. Bloom, D. Hanahan, Differential plasmid rescue from
554 transgenic mouse DNAs into Escherichia coli methylation-restriction mutants., Proc
555 Natl Acad Sci USA. 87 (1990) 4645–4649.
556 [51] R.M.Q. Shanks, D.E. Kadouri, D.P. MacEachran, G.A. O'Toole, New yeast
557 recombineering tools for bacteria., Plasmid. 62 (2009) 88–97.
558 doi:10.1016/j.plasmid.2009.05.002.